THE JOURNAL OF PHYSICAL CHEMISTRY B

Article

pubs.acs.org/JPCB

# On the DMSO-Dissolved State of Insulin: A Vibrational Spectroscopic Study of Structural Disorder

Wojciech Dzwolak,*[,†] Jarosław Kalinowski,[‡] Christian Johannessen,[§] Viktoria Babenko,[†] Ge Zhang,[∥] and Timothy A. Keiderling[∥]

[†]Department of Chemistry, University of Warsaw, Pasteura 1, 02-093 Warsaw, Poland

[‡]Institute of High Pressure Physics, Polish Academy of Sciences, Sokolowska 29/37, 01-142 Warsaw, Poland

[§]Manchester Interdisciplinary Biocentre, University of Manchester, 131 Princess Street, Manchester M1 7DN, United Kingdom

[∥]Department of Chemistry, University of Illinois at Chicago, 845 West Taylor Street (m/c 111), Chicago, Illinois 60607-7061, United States

Supporting Information

**ABSTRACT:** Upon dissolving in dimethyl sulfoxide (DMSO), native insulin and insulin amyloid fibrils convert into an identical disordered structural state based on IR spectral characteristics. Here, we investigate the DMSO-denatured state of insulin using a number of spectroscopic methods: near-UV circular dichroism, infrared absorption spectroscopy, vibrational circular dichroism (VCD), Raman scattering, and Raman optical activity (ROA), as well as by carrying out 140-ns-long molecular dynamics (MD) simulations of DMSO-dissolved native insulin monomers. According to this work, the DMSO-solvated state of insulin is an ensemble of conformations including polyproline II-type helix and possibly a residual $\alpha$-helical structure. Effects of DMSO-specific solvation and conformation-restricting covalent structure of insulin (including the three intact disulfide bridges) are argued to play important roles in stabilizing the disordered state of the protein. A comparison of ROA spectra of insulin dissolved in fully deuterated and nondeuterated DMSO suggested transfer of chirality from the protein to the otherwise ROA-silent solvent. Our study provides an example of a biological protein that acquires a substantial population of PP II conformation in an entirely nonaqueous environment. The DMSO-unfolded state of insulin and its dynamics are also discussed in the context of the established link between PP II conformation and protein misfolding.

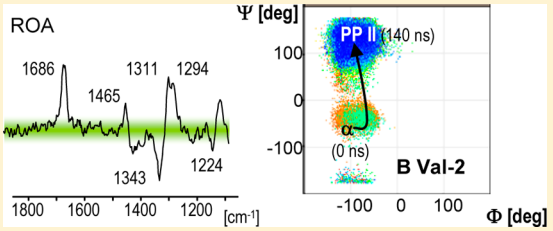


## INTRODUCTION

Transfer of a polypeptide chain from an aqueous milieu into a nonaqueous environment strongly affects its conformation and dynamics.[1] This process is an integral part of the in vivo folding of membrane proteins, and it is also often purposefully induced in vitro in order to gain insight into protein thermodynamics and pathways of the conformational transitions. The capacity of dimethyl sulfoxide (DMSO) to solubilize peptides and to act as a cryoprotector and trans-epidermal carrier of proteins[2] has triggered interest in its biotechnological and pharmaceutical applications[3] and in the physicochemical and conformational characteristics of DMSO-solvated biopolymers.[4−11] In water/DMSO solutions of ribonuclease, lysozyme, $\beta$-lactoglobulin, and chymotrypsinogen, low volume fractions of the organic cosolvent tend to stabilize the native state, which has been explained by the mechanism of preferential hydration.[12] Likewise, low concentrations of DMSO in water have been found to increase the rate of refolding of denatured lysozyme.[13] Destabilizing effects of diluted DMSO are usually confined to dissociation of oligomeric proteins (e.g., refs 14 and 15). At higher concentrations, by contrast, DMSO increasingly reveals a denaturating influence on proteins.[6,9,12] The dependence of a protein's conformational stability on the fractional volume of DMSO is complex, which in part follows from the strongly nonideal behavior of the water/DMSO system.[16−18] DMSO not only perturbs the "microstructure" of water, but since it is a strong H-bond acceptor and a good solvent for apolar side groups, DMSO can also affect a protein through direct binding to its surface. Because of these properties, DMSO has been utilized as an amphipathic membrane-mimicking solvent for certain peptides.[8,11]

Jackson and Mantsch observed that the amide I′ band of the infrared spectra of DMSO-dissolved proteins shifts up in wavenumber to approximately 1663 $cm^{-1}$, indicating that the solvent competes with the main chain carbonyls as an H-bond acceptor leading to formation of free peptide C═O groups.[4] Certainly, such a significant disruption of a protein's native hydrogen bonding pattern would be expected to be accompanied by significant structural disorder. Although it is unclear whether the DMSO-unfolded state has much in common with the disordered protein conformations induced through "conventional" means such as high temperature or

**Received:** June 26, 2012
**Revised:** September 1, 2012
**Published:** September 10, 2012

   dx.doi.org/10.1021/jp3062674 | J. Phys. Chem. B 2012, 116, 11863−11871

chemical denaturants, a study by Kotik et al. showed that the refolding behavior of hen lysozyme after being denatured with either DMSO or guanidine hydrochloride is indistinguishable.[13] A recent NMR study on DMSO-denatured dynein light chain protein suggests that the unfolded form is markedly heterogeneous in terms of the presence of different less-ordered conformations.[10]

A disordered conformation is also formed when amyloid fibrils, the intensively studied aggregated forms of misfolded proteins linked to etiology of several neurodegenerative disorders such as Alzheimer's, Parkinson's, or Huntington's diseases, are dispersed and dissolved in DMSO.[19] An application of DMSO as the ultimate solvent and denaturant for otherwise insoluble and thermodynamically stable protein aggregates has enabled insightful solution NMR studies to be conducted on amyloid fibrils.[20] This is possible due to the fact that the solvent converts large protein aggregates into NMR-accessible monomers, while effectively suppressing undesired H/D-exchange.[21,22] In our previous FT-IR studies, we observed that dissolving either native bovine insulin or insulin amyloid fibrils in DMSO results in the corresponding amide I band being shifted to approximately 1662 $cm^{-1}$.[23−26] Despite insulin's thermodynamic stability and the three disulfide bridges that significantly restrict conformational freedom of its two polypeptide chains (A and B), DMSO instantly converts insulin into a state largely deprived of the native intramolecular hydrogen bonds. Interestingly, when this particular DMSO-induced conformer is used as a starting conformation for insulin refolding in a nonaqueous environment (insulin dissolved in DMSO is rapidly diluted with chloroform which acts as a hydrogen donor competing with the protein backbone in binding to DMSO molecules) the subsequent conformational transition does not end up in the native predominantly $\alpha$-helical state but rather in an anomalous $\beta$-sheet-rich form that is metastable in aqueous environment.[27] Understanding of this unusual behavior requires a deeper insight into what constitutes the DMSO-unfolded state of a protein (and of insulin in particular) reaching beyond the trivialized "coil" paradigm. The highly fluctuating disordered states are inaccessible to most high resolution techniques. Moreover, DMSO strongly absorbs in the far-UV range ruling out applications of electronic circular dichroism (ECD) in the protein-conformation-sensitive wavelength range. Hence, vibrational spectroscopy and molecular dynamics simulations are the methods of choice in the pursuit to elucidate the structural disorder of insulin dissolved in DMSO. In this study, we employ, along with near-UV ECD, FT-IR spectroscopy, and MD calculations, two vibrational chiroptical methods: vibrational circular dichroism (VCD)[28−31] and Raman optical activity (ROA)[32,33] which are conformationally useful biophysical tools that report on protein secondary structure.

## MATERIALS AND METHODS

**Samples.** Insulin from bovine pancreas (Sigma-Aldrich, U.S.A.) was used without further purification. The protein was dissolved at 10 wt % (for ECD, FT-IR, and ROA), or 3 wt % (VCD) concentration in DMSO ("For Molecular Biology" grade from Sigma-Aldrich, U.S.A.), or DMSO-$d_6$ ("99.8 atom % D" grade from ARMAR Chemicals, Switzerland). Deuterated insulin was obtained through solvent exchange of 1 wt % insulin dissolved in $D_2O$ ("99.8 atom % D" grade from ARMAR Chemicals, Switzerland), pD-adjusted to 1.9 (uncorrected readout of the pH-meter) with diluted DCl ("99 atom % D" grade from Aldrich). Acidified insulin samples were solvent-exchanged for 20 min at 65 °C. Subsequently, deuterated protein was precipitated by increasing the pD to 7 with diluted NaOD ("99.5 atom % D" grade from Aldrich; 372072), followed by centrifuging and freeze-drying of the sample. Insulin solutions in DMSO were stable at room temperature for at least two weeks. No association of the protein was observed in the samples, and according to control FT-IR measurements, the protein conformation was the same at either 10 or 3 wt % concentrations.

**ECD Spectroscopy.** Near-UV ECD spectra of insulin dissolved in DMSO and in $D_2O$ at pD 1.9 (at the same concentration as used for FT-IR, 10 wt %) were measured in 0.1 mm quartz cuvettes at 25 °C on a Jasco J-815 S spectropolarimeter, as specified in our previous works.[34]

**FT-IR Spectroscopy.** For FT-IR measurements, a $CaF_2$ transmission cell equipped with a 0.05 mm Teflon spacer was used. The temperature in the cell was controlled through an external water-circuit connected to a programmable thermostat. All FT-IR spectra were collected on a Nicolet NEXUS FT-IR spectrometer equipped with a liquid-nitrogen-cooled MCT detector. Typically, for a single spectrum 256 interferograms of 2 $cm^{-1}$ resolution were coadded. During the measurement, the sample chamber was continuously purged with $CO_2$-free dry air. From each sample's spectrum, corresponding solvent and water vapor spectra were subtracted. Spectra were baseline-corrected and normalized according to integrated intensity of the amide I/I′ band. Data processing (second derivative Savitzky-Golay spectra, peak-fitting with Gaussian/Lorentzian component bands) was performed with GRAMS software (ThermoNicolet, U.S.A.). All further details have been described earlier.[23,27]

**VCD Spectroscopy.** VCD spectra were measured on a homemade dispersive instrument at University of Illinois at Chicago that has been described in detail earlier.[35] Samples were prepared by dissolving insulin in DMSO or DMSO-$d_6$ at a concentration of 3 wt %. Subsequently, each sample was sealed in a homemade transmission cell with $CaF_2$ windows separated by a 0.1 mm Teflon spacer. The spectra were recorded as an average of 8 scans over the amide I′ region, using our standard spectral collection protocols.[31,36] The final spectra were corrected by subtraction of an identically collected spectrum of the solvent. FT-IR spectra were collected on these samples as a control.

**ROA Spectroscopy.** Raman and ROA spectra were collected at ambient temperature on a ChiralRAMAN spectrometer (BioTools, Inc.), which employs the scattered circular polarization measurement strategy in backscattering. The ROA difference spectra are presented as circular intensity differences ($I_R - I_L$) and the parent Raman spectra as circular intensity sums ($I_R + I_L$), with $I_R$ and $I_L$ denoting the Raman-scattered intensities with right- and left-circular polarization states, respectively. Samples were pipetted into quartz micro-fluorescence cells and the measurements were carried out under the following conditions: laser excitation 532 nm, laser power measured at the sample ∼200 mW, spectral resolution ∼7 $cm^{-1}$, and acquisition time ∼30−35 h. Pure solvent spectra were subtracted from the parent Raman spectra, and all spectra were subsequently smoothed using a second level Savitzky-Golay filter.

**MD Simulations.** The starting conformation for the MD simulations was taken from PDB file 2ZP6 of the hexameric bovine insulin determined at 2.56 Å resolution. The simulated

system was an insulin monomer with only the A and B chains retained. Structural comparison with the crystallographic structure of despentapeptide insulin (PDB: 1PID), which exists only in a monomeric form,[37] shows that dimer formation does not lead to significant structural changes, which justifies extracting a monomeric fragment from a complex without further adjustments. The protonation state for the starting configuration was determined using the H++ server (http://biophysics.cs.vt.edu/H++) with default salinity (0.15) and dielectric (80/6) settings, for pH 5.5, which is close to insulin's isoelectric point (5.74) and results in a protonation state with zero net charge. Thus all simulations were performed without counterions, with all termini charged and with −1 charge on Glu and +1 on Arg, Lys, and His residues.[38,39]

Water molecules present in the crystallographic structure and within a 3.6 Å radius from the protein surface (hydrogens were ignored during the test) were preserved. Correct packing of water molecules was set up using Mercury 2.2[40−43] and filtering was performed using MMTK library [44] leaving 15 water molecules. Simulations were performed using periodic boundary conditions. A cubic box of 9.373 nm size containing insulin and 15 adjacent water molecules was filled with equilibrated DMSO solvent (6787 molecules) using the genbox program from the Gromacs package. The simulation time was 140 ns. For the protein and water, Gromos96 (G53a6) and SPC force fields were used. The choice of potentials for the whole system was dictated by the need to obtain a reasonably accurate description of the protein dynamics, giving preference to forcefields designed for proteins over general ones, and, at the same time, to correctly describe properties of bulk DMSO. For the latter purpose there are several potentials available[45−47] in the literature; however, for our system, the parametrization by Geerke et al.[18] was selected as it was specifically designed to be compatible with the Gromos96 force field (for the protein and water part of the system G53a6 variant and SPC force fields were used) and has been tested by Greeke at al. for simulations of thermodynamic properties of bulk DMSO and DMSO−water mixtures (combined with SPC and SPC/L) and also for free enthalpies of solvation for model organic compounds. The model uses a united atom approach with a single interaction site for a methyl group. The S−$CH_3$ bond is elongated (1.938 Å) with respect to distances obtained for S−C from crystallographic measurements (about 1.8 Å) to account for the polarity of methyl groups (see ref 48). The partial charges assigned to S, O, and −$CH_3$ are 0.128, −0.448, and 0.16, respectively.

All simulations were performed using Gromacs version 4.0.7.[49−52] The system (protein, water molecules, and DMSO molecules), with position restraints applied to protein and water heavy atoms, was relaxed using steepest descent minimization (2000 steps) followed by short (2 ps, dt = 2 fs) NVE dynamics simulation. In the following step, position restraints were removed and the system was thermalized in an NVT ensemble (8 ps, dt = 2 fs) using Berendsen thermostat ($T$ = 310 K, $\tau_t$ = 0.1). The production simulation was performed in an NPT ensemble (145 ns, dt = 2 fs) also using Berendsen pressure coupling ($\tau_p$ = 1.0). The value of DMSO compressibility for 298 K, 5.25 × $10^{-5}$ $bar^{-1}$, was used. SHAKE algorithm was applied to constrain bond lengths and also in order to make DMSO molecules rigid.

## RESULTS AND DISCUSSION

**Near-UV Circular Dichroism.** For a protein dissolved in DMSO, the most diagnostically useful spectral range of ECD, which is lying in far-UV, is inaccessible due to the very strong absorption by the solvent. Hence only less useful ECD signals originating from the chiral arrangements of aromatic side chains and disulfide bonds can be accessed in the near-UV region, and this approach was chosen by Hirota-Nakaoka and colleagues to study $\beta_2$-microglobulin dissolved in DMSO.[21] A near-UV CD spectrum of insulin in DMSO is compared with that of the protein in an acidified aqueous environment (favoring dimers with the native secondary and tertiary structure[53]) in Figure 1A.

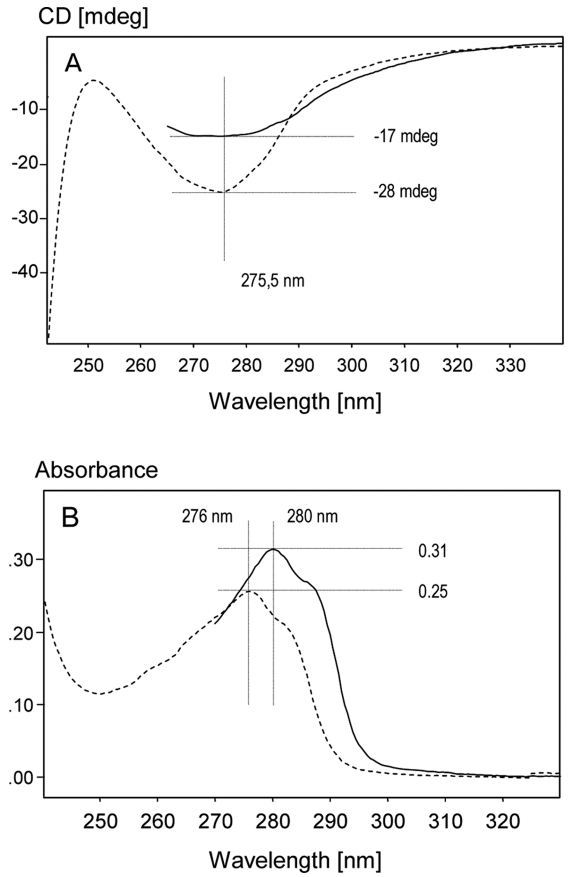


**Figure 1.** (A) Near-UV ECD spectra of nondeuterated insulin in DMSO (solid line) and of native insulin dimers dissolved at pD 1.9 in $D_2O$ (dashed line). (B) The corresponding UV absorption spectra. Low wavelength sides of the spectra of DMSO-based samples have been truncated due to strong light absorption.

The CD signal is dominated by the four tyrosine residues present per insulin monomer. This is reflected by the minimum of ellipticity at approximately 275 nm, whereas contributions from the chiral arrangements of the three phenylalanine residues and three intramolecular disulfide bridges, for which we cannot get data in DMSO, are both expected to appear below 260 nm. Upon the transfer to DMSO, the CD signal of insulin decreases by half and becomes less resolved, implying thereby formation of a less-ordered, at least in terms of tertiary contacts of tyrosine residues, conformation (the spectra in Figure 1 obtained for the DMSO-based and aqueous samples were collected at identical concentrations and optical pathlengths). Interestingly, the corresponding UV-absorption


dx.doi.org/10.1021/jp3062674 | J. Phys. Chem. B 2012, 116, 11863−11871

spectra (Figure 1B) indicate an overall red-shift of the tyrosine band, which, in simplistic terms and in the assumed absence of specific solvent-chromophore interactions, can be interpreted as a typical nonpolar-to-polar (from the protein interior to DMSO) effect on a $\pi-\pi^*$ electronic transition. Thus although lacking deeper structural insights, the near-UV absorption and ECD spectra provide indications of a partial denaturation of the native insulin upon dissolution in DMSO.

**FT-IR and VCD Spectroscopy.** Figure 2A shows infrared absorption along with the corresponding second derivative spectra (inset) of the amide I region of insulin dissolved in DMSO. The shape, width, and position of the amide I band of the protein are distinct from those observed for the native protein or insulin amyloid fibrils.[23,26,27] For proteins dissolved in DMSO, the band's unusual position at approximately 1663 $cm^{-1}$ has been rationalized as a direct consequence of the solvent acting as a powerful H-bond acceptor, forming bonds with the amide N−H groups and resulting in "free" amide C═O groups with higher frequency stretching modes.[4,54] Second derivative spectra and band fitting (shown in Figure 2B) resolve the amide I band into three main individual components, which for the nondeuterated insulin are centered at 1681, 1663, and 1648 $cm^{-1}$. The degree of deuteration-induced red-shift varies and appears to be largest for the 1681 $cm^{-1}$ band. The peak-fitting data suggests that the "free carbonyl" band at ∼1663 $cm^{-1}$ is a minor contributor to the amide I band's overall integral intensity: its prominence being likely caused by the relatively narrow bandwidth rather than other factors (19 $cm^{-1}$ compared to 27 $cm^{-1}$ and 23 $cm^{-1}$ for 1680 and 1650 $cm^{-1}$ bands, respectively, Figure 2B). For a protein dissolved in DMSO, an unequivocal structural assignment of amide I/I′ band is complicated by the fact that its frequency depends not only on the main chain conformation but also on surrounding milieu's dielectric and H-bond-forming properties,[55−58] whereas the spectra-structure reference sets are usually established for crystalline or water-dissolved protein samples.[59] Given the amount of disruption of the native hydrogen bonding pattern, the three individual bands are more likely to represent populations of various local conformations. According to the conventional spectroscopic classification, the 1681 (which appears to be most affected by the H/D-exchange) and ∼1663 $cm^{-1}$ bands fall into the same broad category of those assigned to weakly solvated/solvent-shielded turns.[60]

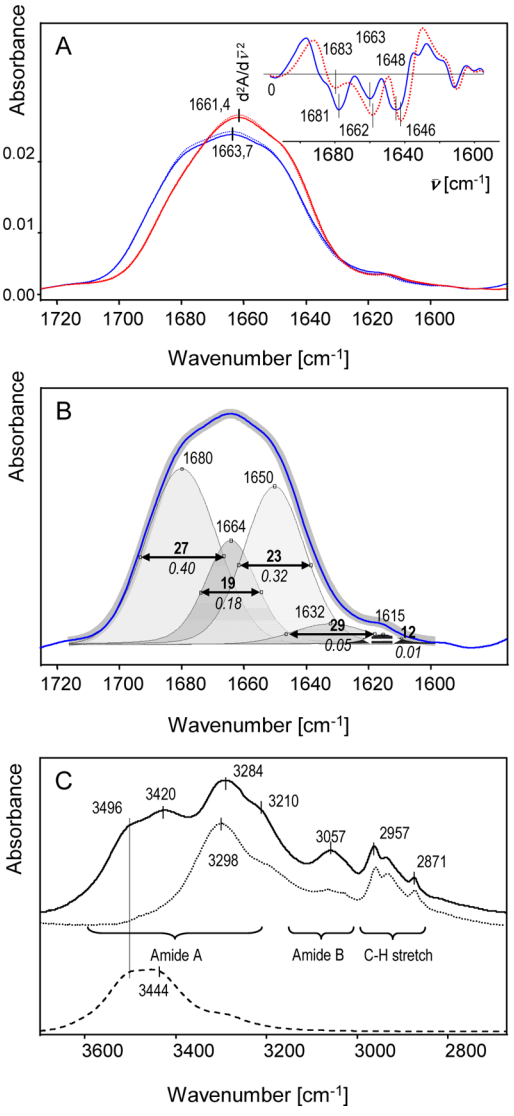


**Figure 2.** (A) Amide I/I′ region of FT-IR absorption spectra of insulin (stock "H" form, blue lines, and deuterated "D" form, red lines) dissolved in nondeuterated DMSO (solid lines) or DMSO-$d_6$ (dotted lines). Inset shows second derivative Savitzky-Golay spectra. (B) Peak fitting of the amide I band of nondeuterated insulin in DMSO with mixed Gaussian−Lorentzian component bands. The blue line denotes the original experimental spectrum, whereas the overlapping thick gray line corresponds to the sum of the component peaks. fwhh is in bold, and relative area under each component band is in italic. (C) Amide A/B region of the infrared spectra of nondeuterated insulin in DMSO-$d_6$ (solvent-subtracted, solid line) and of a dry film of native nondeuterated insulin (dotted line); the dashed line corresponds to solvent-subtracted spectrum of 2.5 v/v % $H_2O$ in DMSO-$d_6$.

In Figure 2C, FT-IR spectra of nondeuterated insulin in the native and DMSO-$d_6$-dissolved states are compared in the wavenumber region encompassing amide A and B bands. The amide A band (dominated by N−H stretches) is sensitive to the degree of hydrogen-bonding of main chain NH groups. Free N−H groups are expected to occur at or above 3495 $cm^{-1}$, whereas the formation of hydrogen bonds shifts the band below 3350 $cm^{-1}$.[61,62] The main 3298 $cm^{-1}$ amide A component of the native insulin is slightly downshifted to 3284 $cm^{-1}$ upon transferring the protein to DMSO-$d_6$. Moreover, it becomes flanked by peaks at higher (3496 and 3420 $cm^{-1}$) and lower (3210 $cm^{-1}$) wavenumbers. Given the position of the O−H stretches of $H_2O$ dissolved in DMSO-$d_6$ (bottom spectrum in Figure 2C), it seems likely that water transferred along with insulin to DMSO-$d_6$ may contribute to the component at 3496 $cm^{-1}$. However, it seems rational to assign the 3420 and 3210 $cm^{-1}$ bands to genuine stretches of free and solvent-bound populations of NH groups, respectively.

We have used VCD and ROA spectroscopy as a complementary approach to this protein conformational problem in nonstandard solvents, since the bandshapes and sign patterns developed are characteristic of conformation and are relatively independent of the frequencies of the underlying vibrational modes. The amide I/I′ region VCD spectra of insulin in DMSO are shown in Figure 3. The spectra are dominated by a negative couplet: positive at 1685 $cm^{-1}$ to negative, and more intense, at 1655 $cm^{-1}$. The VCD couplet shape is very similar to the spectral characteristics of peptides and polypeptides having local conformations approximating a left-handed $3_1$-helix typically associated with the poly(L-proline) II conformation[30,63−69] and that of disordered and denatured


dx.doi.org/10.1021/jp3062674 | J. Phys. Chem. B 2012, 116, 11863−11871

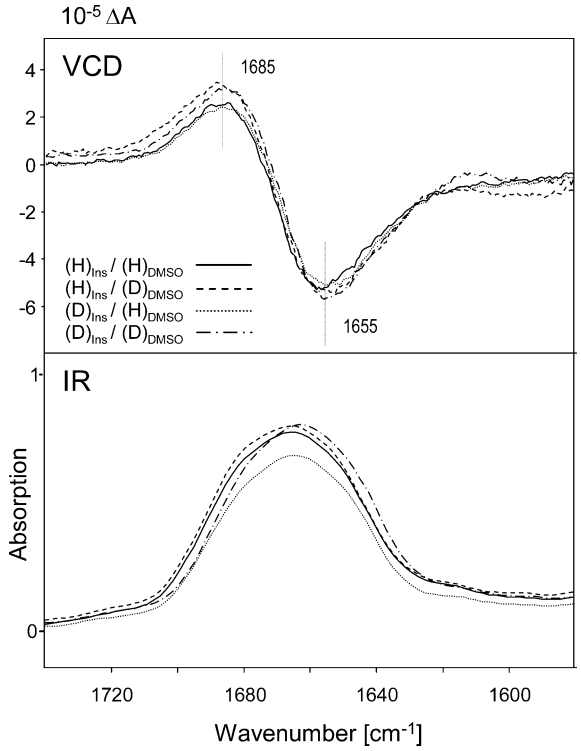


**Figure 3.** VCD and parent infrared absorption spectra of 3 wt % nondeuterated insulin in DMSO (solid line) and in DMSO-$d_6$ (dashed line), and of deuterated insulin in DMSO (dotted line) and in DMSO-$d_6$ (dashed-dotted line).

proteins. However the component frequencies are much higher, again due to the absence of C═O H-bonds in DMSO as compared to the more typical water solvent. Thus VCD suggests that DMSO-dissolved insulin is disordered with a high fraction of PPII like conformation. This VCD band shape is correlated with the central and higher frequency components of the IR band, having been shifted up due to lack of H-bonding as described above. Moreover, the fact that the VCD signal is minimally affected by the deuteration of the backbone (unlike the IR absorption spectra) agrees well with the presence of PPII, as its VCD signature is known to be least affected by deuteration among all major protein conformations.

**Raman and ROA Spectroscopy.** ROA and corresponding Raman spectra of insulin dissolved in DMSO are presented in Figure 4. We have compared spectral effects of deuteration of the protein as well as of the solvent (DMSO replaced with DMSO-$d_6$). The latter step permits examination of the 1350−1450 $cm^{-1}$ region that would otherwise be obscured by bands originating from bending modes of the $-CH_3$ groups of DMSO. A brief survey of the Raman spectra in Figure 4 reveals that deuteration of the solvent has no visible effect, whereas deuteration of the protein itself clearly affects several bands. The amide I band at 1685 $cm^{-1}$ is distinct from the Raman spectra of the known conformational states of insulin: it is strongly upshifted in comparison with the native insulin's band (found at approximately 1662 $cm^{-1}$) and much broader than the sharp 1673 $cm^{-1}$ band prominent in spectra of insulin amyloid fibrils.[69−71] The H/D-exchange causes a minor redshift of the band to 1678 $cm^{-1}$, and it also has a tiny effect in the range of the neighboring overlapping bands of tyrosine and phenylalanine side chains (at 1615 $cm^{-1}$).

The low wavenumber region of the Raman spectra contains conformation-sensitive bands composed of amide III (in-phase N−H deformation and C−N stretch) modes mixed with C$\alpha$H deformations appearing between 1340 and 1200 $cm^{-1}$.[67,72] The lower energy part has greater contribution form the amide III and the higher from the C$\alpha$H, with both having reasonable intensity in Raman yet significant differences in ROA (see below), the latter having a strong positive band at ∼1320 $cm^{-1}$[73] Dissolution of the protein into DMSO is expected to result in a shift of the amide III due to differences in H-bonding from water or internal structures, but the shifts are not established nor easy to predict. As yet, there is no established spectral reference set that would allow one to put forward an unequivocal conformational assignment of the amide III Raman bands shown in Figure 4. The shape and relative intensities of the bands at 1210 (phenylalanine[71]), 1237, and 1267 $cm^{-1}$ are similar to corresponding bands in Raman spectra of native bovine insulin.[71] Hence, according to the Raman data, not much can be ascertained regarding the structural state of insulin in DMSO beyond the rather banal narration of the deuteration-induced spectral changes. The amide I band's position suggests a conformational disorder, whereas the appearance of the amide III bands is inconclusive.

As ROA is known for being more sensitive to protein backbone conformation than conventional Raman scattering,[74] we employed this method to further examine the DMSO-dissolved insulin conformations. The appearance of the amide I band as a single positive band (as opposed to a couplet) at approximately 1690 $cm^{-1}$ suggests again a degree of structural disorder. Also the shape of the couplet in the amide III region (negative at 1340 and a dominant positive ROA at 1309−1313 $cm^{-1}$, Figure 4A) compares to similar spectral signatures detected in the ROA spectra of an amyloidogenic prefibrillar intermediate state of human lysozyme,[75] disordered poly(L-lysine),[76] short alanine oligopeptides,[77] and ovine prion protein,[78] all of which are presently thought of as containing a significant amount of the PP II conformation.[73] The most prominent element of the PP II signature in ROA spectra, the sharp positive band at 1318 $cm^{-1}$ (e.g., refs 73 and 75), is somehow red-shifted in our study (1309 $cm^{-1}$), which could follow from the DMSO-induced dehydration of insulin main chain.[79] However, this line of reasoning must be confronted with the fact that ROA spectra of native insulin in $H_2O$ exhibit a very similar couplet, positive at approximately 1309 $cm^{-1}$ and negative at 1246 $cm^{-1}$ (refs 80 and 81 and Figure S1, Supporting Information) but lack the flanking negative band at 1343 $cm^{-1}$ observed in our study (Figures 4 E, and 4 G). More dissimilarities are visible in the amide I region, which for DMSO-dissolved insulin becomes a single positive band extremely upshifted to ca. 1690 $cm^{-1}$. By contrast, for aqueous samples of the $\alpha$-helical native insulin the band is at 1667 $cm^{-1}$ with a smaller negative neighbor band at 1643 $cm^{-1}$ giving the band a couplet-like appearance.[81]

There is another puzzling aspect of the ROA spectra obtained for the different H/D-isotopic substitution cases shown in Figure 4. As we have stated earlier, deuteration of insulin, unlike deuteration of dimethyl sulfoxide, affects the corresponding Raman spectra. Surprisingly, the opposite seems to be true for the ROA spectra. The H/D-exchange of insulin results in a slight redshift of the amide I band to 1686 $cm^{-1}$, with the region 1170−1200 $cm^{-1}$ becoming somewhat flattened. On the other hand, the DMSO/DMSO-$d_6$ substitution is accompanied by a narrowing of the amide I/I′ band


dx.doi.org/10.1021/jp3062674 | J. Phys. Chem. B 2012, 116, 11863−11871

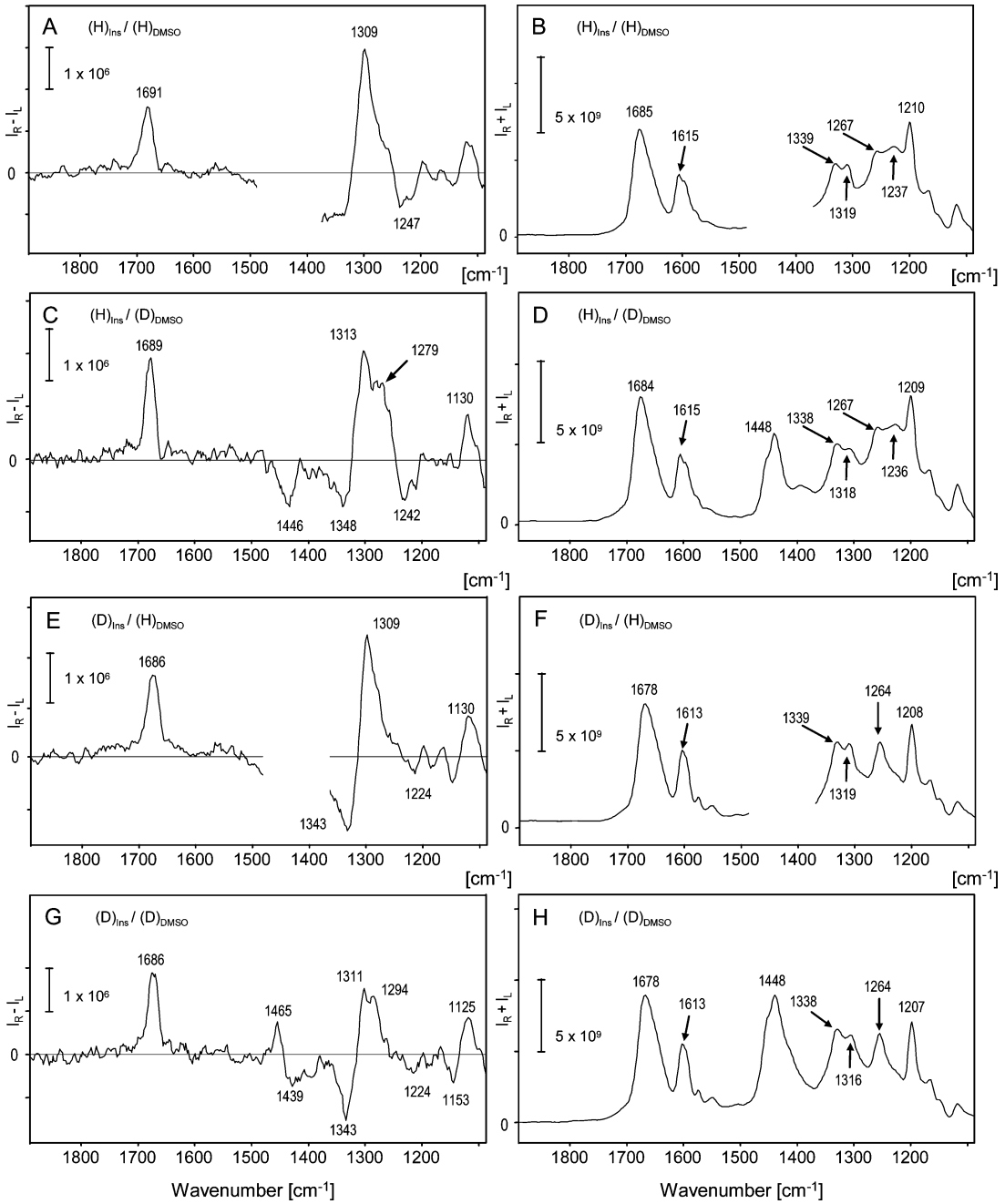


**Figure 4.** ROA (left column, panels A, C, E, and G) and parent Raman (right column, panels B, D, F, and H) spectra of nondeuterated (A–D) and deuterated (E–H) insulin samples in nondeuterated DMSO (A, B, E, and F), and DMSO-$d_6$ (C, D, G, and H). The deleted spectral region in panels A, B, E, and F corresponds to overlapping signals from DMSO's $-CH_3$ groups.

(e.g., Figure 4, panel A vs panel C) and a much more pronounced splitting of the 1309 $cm^{-1}$ band leading to the emergence of a new band below 1300 $cm^{-1}$ (1279 and 1294 $cm^{-1}$ in Figure 4, panels C and G, respectively). Having observed this solvent-induced variation, we have reinspected the corresponding Raman spectra to conclude that along with changes in the ROA, the intensity ratio of the twin 1339/1319 $cm^{-1}$ band is also different depending on the solvent. Mechanisms underlying this unexpected sensitivity of ROA to isotopic substitution in an achiral solvent (which under the conditions of this study does not H/D-exchange with the protein) are not clear. However, given the fact that DMSO (unlike DMSO-$d_6$) has a Raman band at 1309 $cm^{-1}$ (Figure S2, Supporting Information) an induced optical activity due to induced chirality in the protein-bound solvent molecules could be a plausible explanation.[82,83] If that is the case, the ROA spectra collected for DMSO-based samples are partly contaminated by ROA-activated Raman bands of the solvent, and only the spectrum in Figure 4C should be compared to the literature data regarding the ROA signature of PP II conformation. In fact, out of all of the collected ROA spectra, the one shown in Figure 4C is the most characteristic for this conformation.

**MD Simulations.** MD simulations of the temporal evolution of the native insulin conformation (monomer) surrounded by molecules of dimethyl sulfoxide have been run


dx.doi.org/10.1021/jp3062674 | J. Phys. Chem. B 2012, 116, 11863–11871

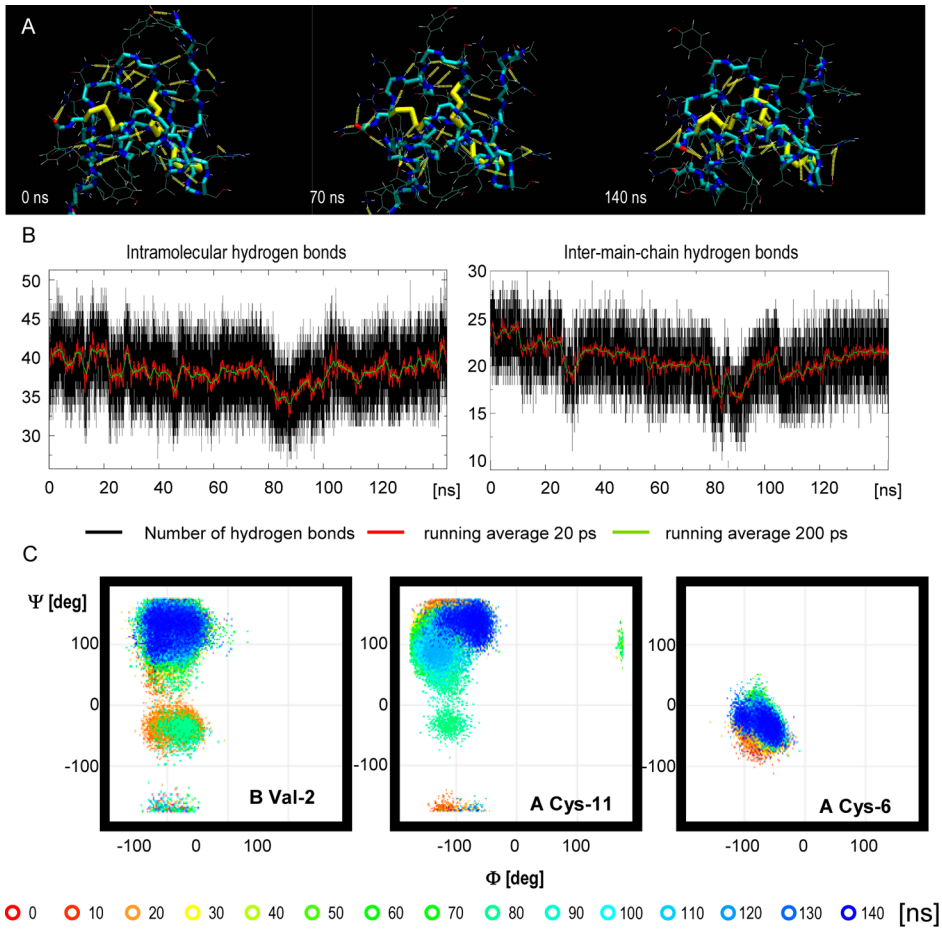


**Figure 5.** MD simulations of insulin in DMSO with residual water. (A) MD snapshots of insulin monomer in DMSO after 0, 70, and 140 ns. (B) Time-dependencies of the total numbers of intramolecular and intermain chain hydrogen bonds. (C) Time evolution of Ramachandran plots of dihedral angles $\varphi$ and $\psi$ for residues Val-2 (B-chain) and Cys-6 and Cys-11 (both of A-chain). The two cysteine side chains form a disulfide bridge, which is assumed to remain intact throughout the conformational transitions of insulin in DMSO. At the bottom, colors are assigned to the different time intervals of the simulation.

for the initial 140 ns. Snapshots after 70 and 140 ns of simulation capture single H-bond-breakage events in the N-terminal part of the B-chain, seen as the upward oriented stretch on the right side of each image in Figure 5A. DMSO is expected to break up native insulin's hydrogen bond network, and the infrared absorption data discussed earlier does support this denaturation scenario, but the MD data collected in this study is more ambiguous. Although water molecules initially solvating ($t$ = 0 ns) the insulin surface are effectively flushed off within the first 7 ns (Figure S3, Supporting Information), changes in the hydrogen bonding patterns are considerably slower. Total transient numbers of intramolecular, and specifically intermain-chain hydrogen bonds are plotted as functions of time in Figure 5B. The dependencies are clearly nonmonotonic, and do not reveal any rapid and cooperative decay of the native hydrogen bonding of insulin. On the other hand, several localized unfolding events are detected when the dihedral angles $\psi$ and $\varphi$ are analyzed. Figure 5C (left panel) depicts a conformational drift from the initial $\alpha$-helical conformation toward PP II ($\psi$ = −78, $\varphi$ = 149 degs) at the Val-2 site of the B-chain. The PP II conformation is also the end state for Cys-11 of the A-chain, although the transition proceeds along a clearly different trajectory and is out-of-phase with the conformational changes at the Cys-6 site of the same chain, both of which form a disulfide bridge in insulin. A time-lapse Ramachandran analysis of the remaining $\psi/\varphi$ pairs along both A and B chains accordingly has been carried out (Figure S4, Supporting Information). Profound conformational changes have been detected at roughly half of all residues within the 140 ns of the MD simulation (13 in the A chain, and 14 in the B chain). Locally, DMSO-induced unfolding leads to populations of different conformations of the main chains, and these include PP II, as well as different types of turns. The picture of the DMSO-denatured insulin emerging from the MD simulation is therefore that of a mixed, partially native-like and partially PP II-like conformation. This would seem in accordance with the spectroscopic characterization of insulin dissolved in DMSO that pointed to the significant amount of the PP II conformation (detected by VCD and ROA, Figures 3 and 4) and possible residual $\alpha$-helical structure (ROA). However, the MD data does not match the experimental results well when it comes to the number of H-bonds broken through the denaturation (Figure 2 vs Figure 5B). It could be hypothesized that the time scale of the MD simulation is too short to access the equilibrated DMSO-solvated insulin state, which was obtained after an hours-long incubation of freshly prepared samples. Hence the MD data is likely to approximate only very early stages of the conformational transitions induced in insulin by DMSO. To say that prolonged protein-DMSO interactions would only promote less ordered states ($\beta$- and $\gamma$-turns, PP II


dx.doi.org/10.1021/jp3062674 | J. Phys. Chem. B 2012, 116, 11863−11871

forming at the expense of the native $\alpha$-helices and $\beta$-strand) would be too simplistic, as the solvent has been shown to promote helical conformation in synthetic peptides.[10,84] Arguably, the relative longevity of insulin's intramolecular hydrogen bonds on the time scale where secondary structural changes already begin to set in is indicative of the fact that DMSO triggers unfolding through more subtle than the H-bond-breaking effects.

## CONCLUSIONS

Upon dissolving in DMSO, insulin acquires a nonhomogenously disordered conformation with significant populations of free main chain carbonyl groups, characterized by a high population of PP II-type conformation, as well as possible residual native $\alpha$-helical structure. Such an ensemble of different conformations may coexist within the small insulin molecule due to conformation-restricting influence of insulin's three disulfide bridges, which remain intact in different conformational forms of insulin,[85] and the DMSO-specific solvation of proteins. Infrared and ROA spectra highlighted a particular aspect of the latter factor consisting in strong H-bond-mediated binding of solvent molecules to main chain N−H groups, leading to the release of peptide's carbonyl groups, and, possibly, inducing optical activity (chiral transfer) in the insulin-bound solvent layer. Our study provides evidence that a biological protein may be forced to acquire PP II−like conformation in an entirely nonaqueous environment. The PP II-like states of many proteins have been linked to their misfolding and amyloidogenic behavior while insulin itself is known for its tendency to form amyloid-like fibrils. However, due to the strong interactions with DMSO, this conformational state is prevented from an imminent amyloidogenesis and remains stable and therefore experimentally accessible for prolonged periods of time. For this reason, further studies on DMSO-induced PP II-states of insulin among other amyloidogenic proteins may be very important for deepening the present understanding of the molecular basis of so-called conformational diseases.

## ASSOCIATED CONTENT

### Supporting Information

Additional ROA, Raman, and MD data. This material is available free of charge via the Internet at http://pubs.acs.org.

## AUTHOR INFORMATION

### Corresponding Author

*Phone: +48 22 8220211 ext. 528. Fax: +48 22 822 5996. E-mail: wdzwolak@chem.uw.edu.pl.

### Notes

The authors declare no competing financial interest.

## ACKNOWLEDGMENTS

This work was supported by the University of Warsaw (501/64-BST-160109 to W.D.) and in part by the U.K. Engineering and Physical Sciences Research Council (C.J.).

## ABBREVIATIONS:

DMSO,dimethyl sulfoxide; DMSO-$d_6$,fully deuterated dimethyl sulfoxide; ECD,electronic circular dichroism; FT-IR,Fourier transform infrared; fwhh,full width at half height; MD,molecular dynamics; PP II,poly(L-proline) II; ROA,raman optical activity; VCD,vibrational circular dichroism

## REFERENCES

(1) Singer, S. J. *Adv. Protein Chem.* **1962**, *17*, 1−68.
(2) Jacob, S. W.; Herschler, R. J.; Bischel, M. *Curr. Ther. Res. Clin. E* **1964**, *6*, 193−198.
(3) Santos, N. C.; Figueira-Coelho, J.; Martins-Silva, J.; Saldanha, C. *Biochem. Pharmacol.* **2003**, *65*, 1035−1041.
(4) Jackson, M.; Mantsch, H. H. *Biochim. Biophys. Acta* **1991**, *1078*, 231−235.
(5) Mierke, D. F.; Kessler, H. *J. Am. Chem. Soc.* **1991**, *113*, 9466−9470.
(6) Iwase, H.; Hirai, M.; Arai, S.; Mitsuya, S.; Shimizu, S.; Otomo, T.; Furusaka, M. *J. Phys. Chem. Solids* **1999**, *60*, 1379−1381.
(7) Burgi, R.; Daura, X.; Mark, A.; Bellanda, M.; Mammi, S.; Peggion, E.; van Gunsteren, W. *J. Pept. Res.* **2001**, *57*, 107−118.
(8) Duarte, A. M. S.; van Mierlo, C. P. M.; Hemminga, M. A. *J. Phys. Chem. B* **2008**, *112*, 8664−8671.
(9) Voets, I. K.; Cruz, W. A.; Moitzi, C.; Lindner, P.; Areas, E. P. G.; Schurtenberger, P. *J. Phys. Chem. B* **2010**, *114*, 11875−11883.
(10) Swagata, C.; Mohan, K. P. M.; Ramakrishna, H. V. *Biochimie* **2012**, *94*, 231−241.
(11) Srivastava, K. R.; Kumar, A.; Goyal, B.; Durani, S. *J. Phys. Chem. B* **2011**, *115*, 6700−6708.
(12) Arakawa, T.; Kita, Y.; Timasheff, S. N. *Biophys. Chem.* **2007**, *131*, 62−70.
(13) Kotik, M.; Radford, S. E.; Dobson, C. M. *Biochemistry* **1995**, *34*, 1714−1724.
(14) Yang, Z. R. W.; Tendian, S. W.; Carson, W. M.; Brouillette, W. J.; Delucas, L. J.; Brouillette, C. G. *Protein Sci.* **2004**, *13*, 830−841.
(15) Visser, N. V.; Wang, D. Y.; Stanley, W. A.; Groves, M. R.; Wilmanns, M.; Veenhuis, M.; van der Klei, I. J. *Arch. Biochem. Biophys.* **2007**, *459*, 208−213.
(16) Luzar, A.; Chandler, D. *J. Chem. Phys.* **1993**, *98*, 8160−8173.
(17) Skaf, M. S. *J. Phys. Chem. A* **1999**, *103*, 10719−10729.
(18) Geerke, D. P.; Oostenbrink, C.; van der Vegt, N. F. A.; van Gunsteren, W. F. *J. Phys. Chem. B* **2004**, *108*, 1436−1445.
(19) Chiti, F.; Dobson, C. M. *Annu. Rev. Biochem.* **2006**, *75*, 333−366.
(20) Hoshino, M.; Katou, H.; Hagihara, Y.; Hasegawa, K.; Naiki, H.; Goto, Y. *Nat. Struct. Biol.* **2002**, *9*, 332−336.
(21) Hirota-Nakaoka, N.; Hasegawa, K.; Naiki, H.; Goto, Y. *J. Biochem.-Tokyo* **2003**, *134*, 159−164.
(22) Hoshino, M.; Katou, H.; Yamaguchi, K. I.; Goto, Y. *Biochim. Biophys. Acta, Biomembr.* **2007**, *1768*, 1886−1899.
(23) Dzwolak, W.; Loksztejn, A.; Smirnovas, V. *Biochemistry* **2006**, *45*, 8143−8151.
(24) Dzwolak, W. *Biochemistry* **2007**, *46*, 1568−1572.
(25) Loksztejn, A.; Dzwolak, W. *J. Mol. Biol.* **2008**, *379*, 9−16.
(26) Loksztejn, A.; Dzwolak, W. *Biochemistry* **2009**, *48*, 4846−4851.
(27) Fulara, A.; Wojcik, S.; Loksztejn, A.; Dzwolak, W. *J. Phys. Chem. B* **2008**, *112*, 8744−8747.
(28) Nafie, L. A. *Vibrational Optical Activity: Principles and Applications*; John Wiley & Sons, Ltd.: Chichester, U.K., 2011.
(29) Polavarapu, P. L. *Vibrational Spectra: Principles and Applications with Emphasis on Optical Activity*; Elsevier: Amsterdam, 1998.
(30) Lakhani, A.; Keiderling, T. A. Conformational Studies of Biopolymers, Peptides, Proteins, and Nucleic Acids. A Role for Vibrational Circular Dichroism. In *Advances in Chiroptical Methods*; Berova, N., Woody, R. W., Polavarapu, P., Nakanishi, K., Eds.; John Wiley: New York, 2012; Vol. 2, Chapter 22, pp 707−758.
(31) Keiderling, T. A.; Kubelka, J.; Hilario, J. Vibrational circular dichroism of biopolymers. Summary of methods and applications. In *Vibrational spectroscopy of polymers and biological systems*; Braiman, M., Gregoriou, V., Eds.; Taylor & Francis: Atlanta, GA; 2006; pp 253−324.
(32) Barron, L. D.; Hecht, L.; Blanch, E. W.; Bell, A. F. *Prog. Biophys. Mol. Biol.* **2000**, *73*, 1−49.
(33) Barron, L. D.; Blanch, E. W.; Hecht, L. *Adv. Protein Chem.* **2002**, *62*, 51−90.
(34) Loksztejn, A.; Dzwolak., W. *J. Mol. Biol.* **2010**, *395*, 643−655.

(35) Lakhani, A.; Malon, P.; Keiderling, T. A. *Appl. Spectrosc.* **2009**, *63*, 775−785.
(36) Lakhani, A.; de Poli, M; Roy, A.; Nakaema, M.; Formaggio, F.; Toniolo, C.; Keiderling, T. A. *J. Phys. Chem. B* **2011**, *115*, 6252−6264.
(37) Ru-chang, B.; Cutfield, S. M.; Dodson, E. J.; Dodson, G. G.; Giordano, F.; Reynolds, C. D.; Tolley, S. P. *Acta Crystallogr.* **1983**, *B39*, 90−98.
(38) Gordon, J. C.; Myers, J. B.; Folta, T.; Shoja, V.; Heath, L. S.; Onufriev, A. *Nucleic Acids Res.* **2005**, *33*, W368−71.
(39) Anandakrishnan, R.; Onufriev, A. *J. Comput. Biol.* **2008**, *15*, 165−184.
(40) Macrae, C. F.; Bruno, I. J.; Chisholm, J. A.; Edgington, P. R.; McCabe, P.; Pidcock, E.; Rodriguez-Monge, L.; Taylor, R.; van de Streek, J.; Wood, P. A. *J. Appl. Crystallogr.* **2008**, *41*, 466−470.
(41) Macrae, C. F.; Edgington, P. R.; McCabe, P.; Pidcock, E.; Shields, G. P.; Taylor, R.; Towler, M.; van de Streek, J. *J. Appl. Crystallogr.* **2006**, *39*, 453−457.
(42) Bruno, I. J.; Cole, J. C.; Edgington, P. R.; Kessler, M. K.; Macrae, C. F.; McCabe, P.; Pearson, J.; Taylor, R. *Acta Crystallogr.* **2002**, *B58*, 389−397.
(43) Taylor, R.; Macrae, C. F. *Acta Crystallogr.* **2001**, *B57*, 815−827.
(44) Hinsen, K. *J. Comput. Chem.* **2000**, *21*, 79−85.
(45) Skaf, M. S. *J. Chem. Phys.* **1997**, *107*, 7996−8003.
(46) Chalaris, M.; Marinakis, S.; Dellis, D. *Fluid Phase Equilib.* **2008**, *267*, 47−60.
(47) Vishnyakov, A.; Lyubartsev, A. P.; Laaksonen, A. *J. Phys. Chem. A* **2001**, *105*, 1702−1710.
(48) Liu, H.; Muler-Plathe, F.; van Gunsteren, W. F. *J. Am. Chem. Soc.* **1995**, *117*, 4363−4366.
(49) Berendsen, H. J. C.; van der Spoel, D.; van Drunen, R. *Comput. Phys. Commun.* **1995**, *91*, 43−56.
(50) Lindahl, E.; Hess, B.; van der Spoel, D. *J. Mol. Model.* **2001**, *8*, 306−317.
(51) van der Spoel, D.; Lindahl, E.; Hess, B.; Groenhof, G.; Mark, A. E.; Berendsen, H. J. C. *J. Comput. Chem.* **2005**, *26*, 1701−1718.
(52) Hess, B.; Kutzner, C.; van der Spoel, D.; Lindahl, E. *J. Chem. Theory Comput.* **2008**, *4*, 435−447.
(53) Whittingham, J. L.; Scott, D. J.; Chance, K.; Wilson, A.; Finch, J.; Brange, J.; Dodson, G. G. *J. Mol. Biol.* **2002**, *318*, 479−490.
(54) Keiderling, T. A.; Silva, R. A. G. D. Conformational Studies of Peptides with Infrared Techniques. In *Synthesis of Peptides and Peptidomimetics*; Goodman, M., Houben-Weyl, G. H., Eds.; Georg Thiem Verlag: New York, 2002; Vol. *22Eb*, pp 715−738.
(55) Ackels, L.; Stawski, P.; Amunson, K. E.; Kubelka. *J. Vib. Spectrosc.* **2009**, *50*, 2−9.
(56) Pattanayak, S. K.; Chowdhuri, S. *J. Phys. Chem. B* **2011**, *115*, 13241−13252.
(57) Grahnen, J. A.; Amunson, K. E.; Kubelka, J. *J. Phys. Chem. B* **2010**, *114*, 13011−13020.
(58) Manas, E. S.; Getahun, Z.; Wright, W. W.; Degrado, W. F.; Vanderkooi, J. M. *J. Am. Chem. Soc.* **2000**, *122*, 9883−9890.
(59) Hadden, J. M.; Chapman, D.; Lee, D. C. *Biochim. Biophys. Acta* **1995**, *1248*, 115−22.
(60) Vass, E.; Hollósi, M.; Besson, F.; Buchet, R. *Chem. Rev.* **2003**, *103*, 1917−1954.
(61) Rozenberg, M.; Shoham, G. *Biophys. Chem.* **2007**, *125*, 166−171.
(62) Du, X.; Liang, Y. *J. Phys. Chem. B* **2004**, *108*, 5666−5670.
(63) Dukor, R. K.; Keiderling, T. A. *Biopolymers* **1991**, *31*, 1747−1761.
(64) Paterlini, M. G.; Freedman, T. B.; Nafie, L. A. *Biopolymers* **1986**, *25*, 1751−1765.
(65) Yasui, S. C.; Keiderling, T. A. *J. Am. Chem. Soc.* **1986**, *108*, 5576−5581.
(66) Chi, H.; Lakhani, A.; Roy, A.; Nakaema, M.; Keiderling, T. A. *J. Phys. Chem. B* **2010**, *114*, 12744−12753.
(67) Schweitzer-Stenner, R. *Vib. Spectrosc.* **2006**, *42*, 98−117.
(68) Keiderling, T. A.; Silva, R. A. G. D.; Yoder, G.; Dukor, R. K. *Bioorg. Med. Chem.* **1999**, *7*, 133−141.
(69) Keiderling, T. A.; Qi, Xu Spectroscopic characterization of Unfolded peptides and proteins studied with infrared absorption and vibrational circular dichroism spectra. In *Advances in Protein Chemistry*; Rose, G., Ed.; Academic Press: New York, 2002; Vol. *62*, pp 111−161.
(70) Dong, J.; Wan, Z. L.; Popov, M.; Carey, P. R.; Weiss, M. A. *J. Mol. Biol.* **2003**, *330*, 431−442.
(71) Mangialardo, S.; Piccirilli, F.; Perucchi, A.; Dore, P.; Postorino, P. *J. Raman Spectrosc.* **2012**, *43*, 692−700.
(72) Herrmann, C.; Ruud, K.; Reiher, M. *ChemPhysChem* **2006**, *7*, 2189−2196.
(73) Zhu, F.; Kapitan, J.; Tranter, G. E.; Pudney, P. D. A.; Isaacs, N. W.; Hecht, L.; Barron, L. D. *Proteins* **2008**, *70*, 823−833.
(74) Barron, L. D.; Zhu, F. J.; Hecht, L.; Tranter, G. E.; Isaacs, N. W. *J. Mol. Struct.* **2007**, *834*, 7−16.
(75) Blanch, E. W.; Morozova-Roche, L. A.; Cochran, D. A. E.; Doig, A. J.; Hecht, L.; Barron, L. D. *J. Mol. Biol.* **2000**, *301*, 553−563.
(76) McColl, I. H.; Blanch, E. W.; Gill, A. C.; Rhie, A. G. O.; Ritchie, M. A.; Hecht, L.; Nielsen, K.; Barron, L. D. *J. Am. Chem. Soc.* **2003**, *125*, 10019−10026.
(77) McColl, I. H.; Blanch, E. W.; Hecht, L.; Kallenbach, N. R.; Barron, L. D. *J. Am. Chem. Soc.* **2004**, *126*, 5076−5077.
(78) Blanch, E. W.; Gill, A. C.; Rhie, A. G. O.; Hope, J.; Hecht, L.; Nielsen, K.; Barron, L. D. *J. Mol. Biol.* **2004**, *343*, 467−476.
(79) McColl, I. H.; Blanch, E. W.; Hecht, L.; Barron, L. D. *J. Am. Chem. Soc.* **2004**, *126*, 8181−8188.
(80) Wen, Z. Q.; Hecht, L.; Barron, L. D. *J. Am. Chem. Soc.* **1994**, *116*, 443−445.
(81) Yamamoto, S.; Watarai, H. *Chirality* **2012**, *24*, 97−103.
(82) Nicu, V. P.; Debie, E.; Herrebout, W.; Van der Veken, B.; Baerends, E. J.; Bultinck, P. A *Chirality* **2010**, *21*, S287−S297.
(83) Debie, E.; Bultinck, P.; Herrebout, W.; van der Veken, B. *Phys. Chem. Chem. Phys.* **2008**, *10*, 3498−508.
(84) Brewer, D.; Howard, H.; Gilles, L. *Biochem. Cell Biol.* **1998**, *76*, 247−256.
(85) Kurouski, D.; Washington, J.; Ozbil, M.; Prabhakar, R.; Shekhtman, A.; Lednev, I. K. *PLoS One* **2012**, *7*, e36989.